Critical Point and Metal-Nonmetal Transition in Expanded Liquid Metals

Helmut Hess[a]; Hartmut Schneidenbach[a]; Andreas Kloss[a]
[a] Institute of Low-Temperature Plasma Physics, Greifswald

PLEASE SCROLL DOWN FOR ARTICLE

CRITICAL POINT
AND METAL–NONMETAL TRANSITION
IN EXPANDED LIQUID METALS

HELMUT HESS*, HARTMUT SCHNEIDENBACH
and ANDREAS KLOSS

*Institute of Low-Temperature Plasma Physics,
Robert-Blum-Strasse 8 – 10, D-17489 Greifswald*

For most metals the two phases of the liquid–gas transition are metallic in a region around the critical point. A method for determining the critical data of expanded liquid metals under such conditions has been published recently. Mercury, however, is a well-known exception with the metal–nonmetal transition inside the liquid phase. Mercury is no longer a metal at the critical point. The metal–nonmetal transtion of the metallic elements has been considered in view of this problem. It is shown that a group of metals (Mg; Zn, Cd; As, Sb; Se, Te), including semi-metals as well, should also have the metal–nonmetal transition completely inside the liquid phase. Thus, the above mentioned method is not applicable in this group. A comparison of the measured electrical conductivity of Al, W, Zn, and Hg with a theoretical approach supports this conclusion.

1. INTRODUCTION

Despite the urgent demands of high-power technology, there is a remarkable lack of knowledge about the state of metals around their critical points. Critical data, *e.g.*, have been measured with a high accuracy only for mercury and for the heavier alkali metals potassium, rubidium and caesium (Hensel [1]; Hohl [2]). For sodium, the measurements differ widely, and for lithium there have not been any

---

*Corresponding author.

experiments so far. For other metals there have been very few first experimental approaches to this subject, mainly by pulse experiments (Hodgson [3]; Seydel, Fucke and Wadle [4]; Pottlacher [5]; Martynyuk [6]; Hess, Kaschnitz and Pottlacher [7]). Thus, the present knowledge of the metal critical data mainly results from rough estimations using different "rules" based on thermodynamic properties of the substances far away from the critical point. Alternatively, in the case of plasma-like critical points, Likalter [8, 9] has derived approximate similarity laws for the critical parameters itself which only depend on atomic characteristics, i.e., the valence and the ionization potential. The background of the similarity is the universality of the Coulomb interparticle interaction. Unfortunately, the value of the valence at the critical point is usually not known except in simple cases like alkali metals. This value has been extracted by Hess [10] combining Likalter's similarity laws with a parametrized vapor pressure curve. Clearly, the latter is constructed in general with low-temperature vapor-pressure data introducing by part the above mentioned uncertainties. The method has been used for the estimation of the critical data of transition metals [11].

It can be assumed that most metallic elements have plasma-like critical points. The alkali metals rubidium and caesium, e.g., have a metallic electrical conductivity slightly above $200 \, \Omega^{-1} \mathrm{cm}^{-1}$ at the critical point [12]. A similar behavior can be seen for copper [13, 14], for aluminium [15, 39] and for tungsten [16]. Mercury [1], however, already shows in the fluid phase with decreasing density a sharp decrease of the electrical conductivity down to about $1 \Omega^{-1} \mathrm{cm}^{-1}$ at the critical point: mercury is no longer a metal and its critical data do not follow Likalter's similarity laws. Thus, the critical point of metals cannot be analyzed without considering its relation to the metal – nonmetal transition. Even in the case of plasma-like critical points the vicinity of the metal – nonmetal transition results in a strong electron-ion coupling which controls the character of the phase transition [8, 9]. The metal – nonmetal transition itself is properly described by a percolation model because of the disordered structure of expanded liquid metals [17, 18].

The plasma-like character of the critical point is a basic condition for Likalter's theory but not a result. The knowledge of the realization of this condition is required. The estimation of both, the critical data according to Hess [10] as well as the density of the metal – nonmetal

transition point according to Likalter [22], is used to get this information. Indeed, most metals seem to remain metallic at their critical points, but some elements show a mercury-like behavior: the alkaline-earth metal magnesium (but not beryllium, strontium and barium; no data about calcium), the metals of the IIB group zinc and cadmium (and mercury itself), further the semi-metals arsenic and antimony of the VA group (no information about bismuth), and finally selenium and tellurium of the VIA group. For selenium, there already exists an experimental hint about a very low electrical conductivity at its critical point [19, 20].

A comparison of theoretical and experimental values of the electrical conductivity for zinc, tungsten, aluminum and mercury supports the reliability of the used theoretical approach. The most recent conductivity data [21] of zinc show a tendency to a mercury-like behavior.

2. METAL–NONMETAL TRANSITION POINT
    AND CRITICAL DATA

In contrast to liquid metals near the melting line the metals near the critical point of the liquid–gas phase transition, the expanded metals, show a gas-like disorder [18]. Approaching the neighboring metal–nonmetal transition from low densities, metallic clusters of different scales are formed. The screening of the metal atoms in the clusters can be described in general by semi-classical valence electrons. Thus, the touch of classically accessible spheres of the valence electrons in ground state atoms with the radius $R_a = e^2/I$ is a necessary condition for a metallic cluster state (e is the electron charge and I is the first ionization potential of the atom). This defines a percolation problem for overlapping spheres [18] and the corresponding characteristic parameter is the classically accessible volume fraction $\zeta = (R_a/R_s)^3$ with the Wigner-Seitz radius $R_s = (4\pi n_i/3)^{-1/3}$ and the ion density n_i. The percolation threshold, e.g., the formation of an infinite percolation cluster, takes place at $\zeta_{th} \approx 1/3$ and

$$n_{th} = \frac{3}{4\pi} \cdot \zeta_{th} \cdot \left(\frac{I}{e^2}\right)^3 = 7.99 \cdot 10^{19} \zeta_{th} \cdot \left(\frac{I}{eV}\right)^3 cm^{-3} \qquad (1)$$

is the corresponding density. Obviously, this threshold can be iden-
tified with the metal–nonmetal transition point [22]. The value used in
the following is $\zeta_{\text{th}} = 0.29$ which fits the metal–nonmetal transition
point of mercury.

According to Likalter [9], in the metallic liquid near the metal–
nonmetal transition point a virtual atomic structure is maintained and
the electron-ion interaction plays the dominant role. The interaction
energy is not pair-additive. The energy per atom saturates and the role
of fluctuations diminishes with increasing average number of the
nearest neighbors with overlapping classically accessible spheres. A
cell model can be used for the description of the interaction. In the
limit of high coordination number $N_c \sim (2R_a/R_s)^3 \gg 1$ the electron
density becomes almost uniform in the atomic cell, and the interatomic
interaction energy has the Madelung form

$$u = -\gamma \, n_i \frac{z^2 e^2}{R_s} \tag{2}$$

with a renormalized Madelung coefficient $\gamma \approx 1/3$ and z is the number of
valence electrons per atom. A limited coordination number has
been taken into consideration by Likalter with an expansion of u on
the small parameter $R_s/2R_a \sim N_c^{-1/3}$ up to the quadratic term where
Eq. (2) is the first term of the expansion. For the construction of a three-
parameter equation of state, in addition to this attractive interaction,
responsible for the elastic pressure, a hard sphere model is used for the
thermal pressure assuming a constant value for the ratio of the hard
sphere radius to the classically accessible radius. An application of this
equation of state on the vicinity of the critical point and fitting the
critical parameters of cesium results in the general scaling laws [9]

$$\frac{n_{ic}}{\text{cm}^{-3}} \approx 2.92 \cdot 10^{19} \cdot \left(\frac{I}{\text{eV}}\right)^3 \quad kT_c \approx 0.0425 \cdot z_c \cdot I,$$

$$\frac{p_c}{\text{MPa}} \approx 0.0405 \cdot z_c^2 \cdot \left(\frac{I}{\text{eV}}\right)^4 \tag{3}$$

and a simple relation between p_c and T_c with eliminated z_c

$$\frac{p_c}{\text{MPa}} = 22.5 \cdot \left(\frac{I}{\text{eV}}\right)^2 \left(\frac{kT_c}{\text{eV}}\right)^2 \tag{4}$$

for plasma-like critical points where k is the Boltzmann constant and n_{ic}, T_c, p_c, z_c are the ion density, the temperature, the pressure and the valence at the critical point, respectively.

Both, the density at the metal–nonmetal transition point and the critical density depend only on the ionization potential and their ratio

$$\frac{\rho_{th}}{\rho_c} = \frac{n_{th}}{n_{ic}} \approx 2.74 \cdot \zeta_{th} < 1 \qquad (5)$$

is a general constant for all metals with plasma-like critical points where ρ is the mass density.

According to Hess [10] the actual values of p_c and T_c can be extracted from the known temperature dependence of the vapour pressure $p_v(T)$ and Eq. (4)

$$p_v(T_c) = p_c(T_c). \qquad (6)$$

Then the critical valence z_c^v follows from Eqs. (3) where the upper label v symbolizes the use of Eq. (6). The parametrized vapour pressure equation

$$\ln(p_v) = A + B/T + C \cdot \ln(T)$$

is used for the extrapolation of data given by Hultgren et al. [24]; Kubaschewski, Alcock and Spencer [25] and Iida and Guthrie [26]. Besides cesium on which the scaling laws are fitted the method excellently works in the case of heavier alkali metals [10]. Obviously, the extrapolation causes uncertainties if data are available only far away from the critical point. Even though experimental critical data for the majority of metals are not available, in some sparse cases the valence at the critical point is expected to have well-defined values and Table I shows a comparison with the calculated ones. The reliability of both, the scaling laws in the case of poly-valent simple (Be, Al) and transition metals (Cu, W) as well as the vapour pressure curves, is supported by the results. Apparently, mercury is an exception in Table I. The density at the metal–nonmetal transition point as well as the critical data are available from highly accurate experiments of the Hensel group (Götzlaff [28]). Mercury is the classical example of a liquid metal for densities down to the metal–nonmetal transition point at $\rho_{th} = 8.8\,\text{g/cm}^3$ and the percolation

TABLE I   Critical valence z_c equal to the oxidation number for the simple metals Be and Al and for the transition metals Cu and W according to Likalter [9, 27], z_c^v in column 2 is z_c from Eqs. (3) with p_c or T_c from Eq. (6), columns 3 to 5 show the mass density at the metal–nonmetal transition point (Eq. (1) with $\zeta_{th} = 0.29$) and at the critical point (Eq. (3)) as well as the ratio of the critical density to the normal solid state density ρ_s. The experimental values for mercury are taken from the Hensel group [1, 28, 32]

Metal	z_c	z_c^v	$\rho_{th}/g\ cm^{-3}$	$\rho_c/g\ cm^{-3}$	ρ_c/ρ_s
Be	2	1.92	0.280	0.353	0.19
Cu	2 [9]	2.00	1.13	1.42	0.16
Al	3	3.08	0.223	0.280	0.10
W	3 [27]	3.14	3.59	4.52	0.23
Hg		**0.25**	8.8	**11.0**	0.81
			≳9 [1, 32]	5.8[28]	0.43

threshold can be fitted on this value to be $\zeta_{th} = 0.29$ [22]. The critical density $\rho_c = 5.8\,g/cm^3$, however, is smaller than ρ_{th}. Thus, the critical point does not have plasma-like character. The scaling laws Eq. (3) are not applicable which is reflected by the mercury results in Table I. Even though Likalter's theory does not answer the question for the condition of a plasma-like critical point, nevertheless the unrealistic high critical density and especially the unphysical value smaller than one for the critical valence from Eqs. (6, 3) seem to be indicators for the violation of this condition.

The success of the percolation model in the case of the heavier alkali metals and the results of Table I as well as the clear hints for deviations in case of mercury advise a further inspection of metals throughout the periodic system. Correspondingly the two quantities z_c^v shown in Figure 1 and the ratio ρ_{th}/ρ_s shown in Figure 2 are considered where ρ_s is the normal solid state density. Additionally in Figure 1 the critical valence z_c^{Gu} is given which results from Eq. (3) with estimated critical temperatures with the so-called Guldberg rule [10]

$$T_c^{Gu} \approx 2.07 \cdot T_b \qquad (7)$$

where T_b is the boiling temperature at atmospheric pressure. There is a group of metals included in Table II (Mg, Zn, Cd, As, Sb, Se, Te) for which both, z_c^v and z_c^{Gu}, are smaller than unity like for mercury.

Whereas the critical valence z_c^v is a more or less artificial quantity in the cases beyond the range of validity of the underlying theory, the density for the metal–nonmetal transition point Eq. (1) follows from
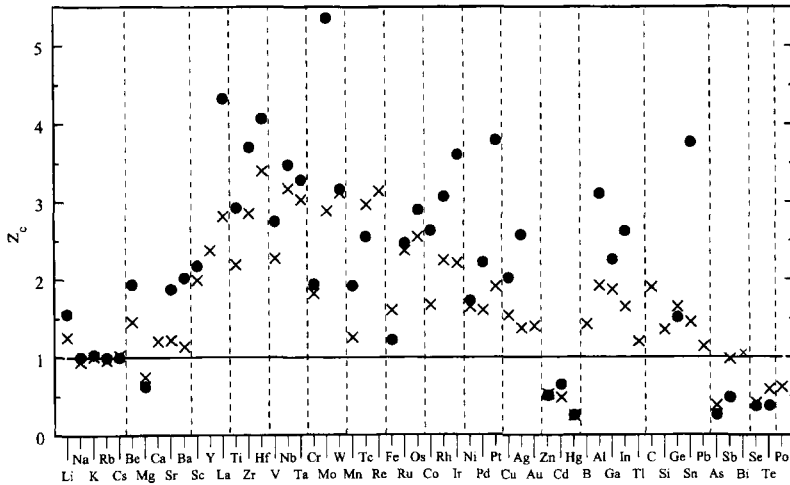
FIGURE 1   Critical valence z_c *versus* the metals throughout the periodic system, $\bullet$ z_c^v from Eq. (3) with p_c or T_c from the vapor-pressure equation (Eq. (6)), $\times$ z_c^{Gu} from Eq. (3) with T_c estimated with the so-called Guldberg rule (Eq. (7)).

TABLE II   Main oxidation number v, critical valence z_c^v, mass density at the metal–nonmetal transition point ρ_{th} (Eq. (1)) and the critical density ρ_c from different sources

Metal	v	z_c^v	$\rho_{th}/g\,cm^{-3}$	ρ_c/gcm^{-3}	
				from different sources	*Eq. (9)*
Mg	2	0.77	0.418	0.41^a , 0.38^b , 0.46^d , 0.56^e , 0.53^k	0.35...0.58
Zn	2	0.50	2.08	2.4^b , 2.0^d , 2.3^e , 2.2^k , 2.6^m	1.4...2.4
Cd	2	0.64	3.14	2.8^b , 2.3^d , 2.7^e , 2.8^k	1.7...2.9
Hg	2	0.25	8.77	4.8^b , 5.3^c , 3.9^d , 5.7^e , $\mathbf{5.8}^i$ 5.0^k	<2.7...4.5
As	3	0.26	2.72	2.6^g	1.2....1.9
Sb	3	0.48	3.02	1.9^d , 2.6^e	1.3...2.2
Se	4	0.37	2.82	1.6^e , 1.2^f , 2.0^h , 1.2^k	1.0....1.6
Te	4	0.37	3.59	2.2^e	1.3...2.1

[a]Mc Gonigal, 1962 [30]; [b]Morris, 1964 [31]; [c]Hensel, 1966 [32]; [d]Young, 1971 [33]; [e]Fortov, 1974 [34]; [f]Rau, 1974 [35]; [g]Alekseev, 1975 [36]; [h]Fischer, 1980 [37]; [i]Götzlaff, 1988 [28]; [k]Martynyuk, 1989 [38]; [m]Pottlacher, 1995 [5].

comparatively simple and quite general considerations applicable for all metals. According to Eq. (5) with $\zeta_{th} = 0.29$ the critical density should be higher by a factor of ≈ 1.26 for metals with plasma-like critical point. On the other hand some crude limits can be estimated for ρ_c. While the alkalis potassium, rubidium and caesium expand by a factor of 5 (compared with solid density at 1 bar), the nonmetallic rare

gases neon, argon, krypton and xenon, for instance, only expand by a factor of 3 (compared with solid density at the triple point):

$$\text{Alkalis: } \rho_c \cong (0.20 \pm 0.01) \cdot \rho_s,$$
$$\text{Rare gases: } \rho_c \cong (0.32 \pm 0.01) \cdot \rho_s. \tag{8}$$

Thus, nonmetals show a lower expansion from the solid to the critical point than metals for which Young [29] has given the simple rule

$$\rho_c \approx (1/5 \ldots 1/3) \cdot \rho_s. \tag{9}$$

If $\rho_{c,\text{max}} \approx \rho_s/3$ is chosen as the upper limit for the critical density of metals, the upper limit for the density at the metal–nonmetal transition point

$$\rho_{\text{th,max}} \approx 0.26 \cdot \rho_s \tag{10}$$

follows from Eq. (5) with $\zeta_{\text{th}} = 0.29$. Interestingly, in Figure 2, except Mg, the group of metals with $z_c^v < 1$ has densities ρ_{th} well above the limit given by Eq. (10), too. Additionally, this behavior is also shown
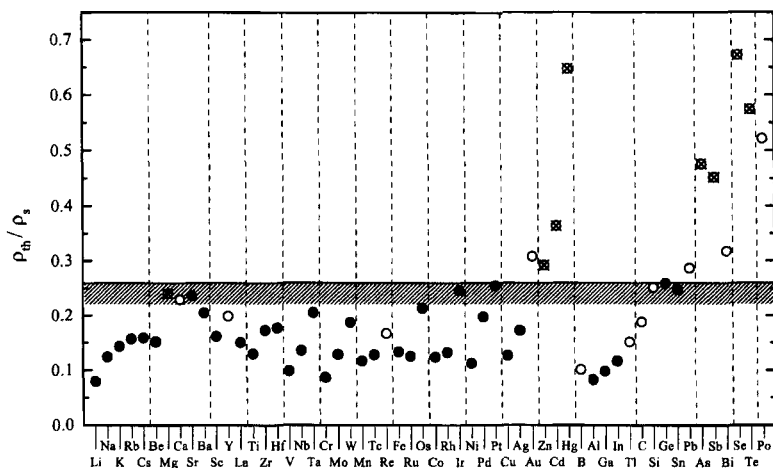

FIGURE 2   Ratio of the density at the metal–nonmetal transition point (Eq. (1)) to the normal solid state density ρ_{th}/ρ_s *versus* the metals throughout the periodic system, ● $z_c^v \geq 1$, ⊗ $z_c^v < 1$, ○ z_c^v- could not be extracted, where z_c^v is the critical valence from Eq. (3) with p_c or T_c from the vapor-pressure equation (Eq. (6)). The upper boundary of the dashed area corresponds to $\rho_c = \rho_s/3$.

by Au, Pb, Bi and Po for which z_c^v could not be extracted. Mg is included in a second group (Mg, Ca, Sr, Ir, Pt, Si, Ge, Sn) with densities ρ_{th} near the limit.

3. ELECTRICAL CONDUCTIVITY OF ZINC

The decisive role played by the metal – nonmetal transition in the discussion of the critical point of metals is shown above. It is suggested to analyze this transition itself with a comparison of theoretical and experimental values of the electrical conductivity in the relevant parameter range.

In the virtual atomic structure near the metal – nonmetal transition point the atoms represent complex quasiparticles. For the determination of the diffusion and mobility of electrons the internal energy spectrum of these quasiatoms as well as the density of states have to be discussed. Percolation results in a virtual screening of the ions and an asymptotically free valence electron motion becomes possible. Hence, the internal energy spectrum of the quasiatoms counting from the ion core energy [22]

$$E_p = -I + \varepsilon_p, \quad \varepsilon_p = \frac{p^2}{2m} \tag{11}$$

contains a continuous part where ε_p is the electron excitation energy, p is the electron momentum far away from the screened ion core and m is the electron mass. Equation (11) is written for simplicity for one-valent atoms, only. The admixture of free motion is small for weak excitations. Thus, the transition time τ' of an electron to a neighboring virtual hole, e.g., for localization at a new ion, is correspondingly larger than the gaskinetic relaxation time τ. The sphere for counting the distinguishable quasiatomic states has the radius $v \cdot \tau'$ with $v = v_T$ and $v_T = (8kT/\pi m)^{1/2}$ is the mean thermal velocity. Introducing the localization factor $\vartheta = \tau/\tau'$ this sphere as well as the density of states are larger by a factor of ϑ^{-3} and the Fermi energy in the case of s valence electrons is smaller by a factor of ϑ^2 than the corresponding quantity of a homogeneous electron gas. For a well established virtual atomic structure, e.g., for small ϑ values, the ratio of the Fermi energy to a temperature in the order of the critical one is small and Boltzmann

statistics becomes applicable. Moreover, the localization sphere is much larger than the sphere for ion potential screening and in good approximation the density of states in the quasiatom is represented by that of a nearly-free electron gas.

The electron transitions to virtual holes result in a diffusion with a coefficient $D_e = \ell^2/(3\tau') = \vartheta \cdot \ell v/3$ and the mobility becomes $\mu = \vartheta \cdot e\tau/m$, e.g., the gaskinetic quantities are multiplied by the localization factor [22]. According to the principle of Joffe and Regel [23] the mean free path ℓ in the gaskinetic case cannot be smaller than the mean interatomic distance. Further decrease results in localization. Thus, $\ell = R_s$ can be chosen in the range of percolation mobility. It is left to calculate ϑ.

Obviously, below the percolation threshold $\zeta_{th} \approx 1/3$ nonzero mobility is only possible with excited quasiatoms, the classically accessible radius of which $R_a(\varepsilon) = e^2/(I - \varepsilon)$ increases with ε. With the corresponding ε-dependent classically accessible volume fraction the mobility gap in the range of partial localization is defined by the two excitation energies [22]

$$\zeta(\varepsilon) = \left(\frac{R_a(\varepsilon)}{R_s} \right)^3 = \zeta_j, \quad \Delta_j = I - e^2 \left(\frac{4\pi n_i}{3\zeta_j} \right)^{1/3}, \quad j = 1, 2. \quad (12)$$

For $\varepsilon < \Delta_1$ with $\zeta_1 = \zeta_{th} \approx 1/3$ the mobility is zero. The second value $\zeta_2 \approx 2/3$ corresponds to randomly closed-packed quasiatoms and characterizes the boundary of the gaskinetic case. Percolation mobility takes place for $\Delta_1 \leq \varepsilon \leq \Delta_2$.

Based on arguments of the scaling theory of localization, for the mobility a linear dependence on the excitation energy above the threshold up to the gaskinetic limit is assumed. Finally, the average of the mobility, normalized by its gaskinetic limit, over the Boltzmann distribution results in the explicit expression [22]

$$\vartheta = kT \frac{F_1 - F_2}{\Delta_2 - \Delta_1} \quad (13)$$

for the localization factor where $F_k = (2/\sqrt{\pi})[\Gamma(5/2, \Delta_k/kT) - (\Delta_k/kT)\Gamma(3/2, \Delta_k/kT)]$ contains the incomplete gamma-functions $\Gamma(a, z)$.

Finally, the electrical conductivity is given by a modified Drude formula

$$\sigma = \frac{e^2 n_e \tau}{m} \cdot \vartheta \tag{14}$$

where n_e is the electron density and $\tau = \ell/v_T$ with the Joffe-Regel minimum $\ell = R_s$. With decreasing temperature or increasing density electron degeneracy increases. In the case of strong electron degeneracy the percolation character of the conductivity is lost and the mean free path becomes larger than R_s [22]: $\tau\vartheta \rightarrow \ell/v_F$ where v_F is the Fermi velocity. Matching of the Boltzmann conductivity with the degenerate one *via* $v_T = \gamma_F \cdot v_F$ results in $\ell = R_s/\gamma_F$. γ_F is a coefficient in the order of unity which can be extracted from the electrical conductivity near the melting point [22].

Figure 3 shows the results of Likalter's theory in comparison with experimental data for zinc [21], tungsten [16], aluminum [15, 39] and mercury [28]. The electrical conductivity, relative to the conductivity at the melting point, has been given in dependence on the density, relative to the normal solid state density. From the simple model for the gaskinetic relaxation time τ only a qualitative description of the experiment can be expected . For dense metals near the melting point the well-known Ziman formula is more appropriate. Generally a consistent quantum statistical approach [40] has to be used for a quantitative description in the gaskinetic case. Thus, the theoretical curves have been only drawn for the transition region. Additionally, the σ values from Eq. (14) have been adjusted by multiplying with factor 1.6 for Zn, 0.47 for W, 0.42 for Al and 1.0 for Hg. The temperature has been chosen in accordance with the conditions in the transition region in the corresponding experiment. Obviously, the transition is broadened with increasing temperature, but the form of the density dependence of σ is rather insensitive in the relevant temperature range. The good qualitative agreement with the experiment supports the reliability of the expanded liquid metal theory, underlying the critical data analysis in the present paper. The metal – nonmetal transition points Eq. (1) are marked by open squares in Figure 3. Apparently, the decrease of the electrical conductivity of zinc is shifted to higher relative densities with respect to aluminum and tungsten. The high theoretical ρ_{th} seems to be a realistic value.
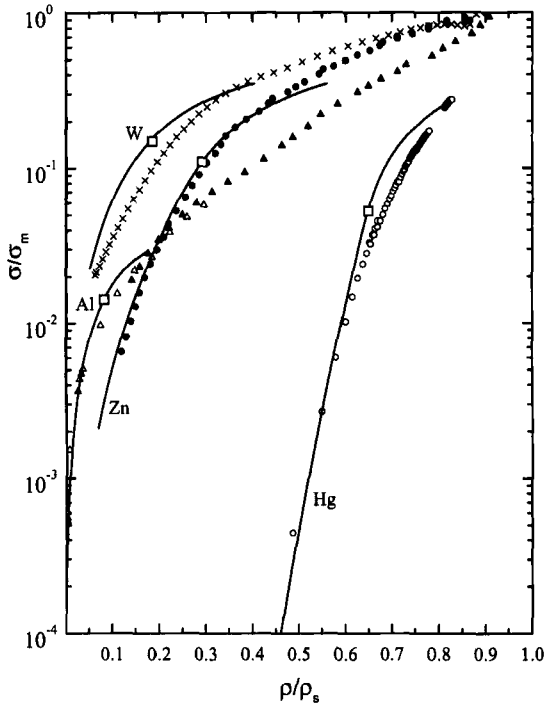
FIGURE 3   Ratio of the electrical conductivity to the conductivity at the melting point σ/σ_m versus the ratio of the density to the normal solid state density ρ/ρ_s, experiment: × tungsten [16], ● zinc [21], ▲ aluminum (Kloss et al. [39]), △ aluminum (Krisch et al. [15, 39]), ○ mercury [28], theory: Solid lines for σ/σ_m from Eq. (14) multiplied by a factor 1.6 for Zn, 0.47 for W, 0.42 for Al and 1.0 for Hg, the open squares label the metal–nonmetal transition points according to Eq. (1).

4. DISCUSSION AND SUMMARY

In the case of plasma-like critical points of the liquid – gas phase transition of metals, approximate similarity laws for the critical parameters have recently been derived by Likalter. These relations only depend on atomic characteristics, i.e., the valence and the ionization potential. A strong electron-ion coupling, caused by the near metal–nonmetal transition, controls the character of the phase transition. The basic assumption of a plasma-like critical point is not fulfilled for mercury. The density at the metal – nonmetal transition

point is higher than the critical one, and the similarity relations are violated. The metals throughout the periodic system have been inspected in view of this question. With an extrapolated vapor pressure curve the critical valence can be extracted. A group of metals (Mg, Zn, Cd, Hg, As, Sb, Se, Te) show unphysical critical valences smaller than unity. Both a violation of the similarity laws or an incorrect extrapolation of the vapor-pressure curves can be the reason. But, a second criterion results from the theory which gives a fixed relation between the critical density and the density for the metal – nonmetal transition point. Contrary to the critical density the theoretical value of the latter holds quite general for all metals. Indeed, except Mg, the same group of metals shows the metal – nonmetal transition at densities well above a properly chosen upper limit for plasma-like critical points. Additionally, this behavior is also shown by Au, Pb, Bi, and Po for which the critical valence could not be extracted. A second group (Mg, Ca, Sr, Ir, Pt, Si, Ge, Sn) has densities near the limit.

Finally, the comparison of the measured electrical conductivity for zinc, tungsten, aluminum and mercury with Likalter's theory gives good qualitative agreement. For zinc the high density of the metal – nonmetal transition point as well as the tendency to a mercury-like behavior are confirmed.

References

[1] Hensel, F. (1987). In: *Large Finite Systems*, (Eds.) Jortner J. *et al.* (D. Reidel Publishing Company), pp. 345–359.
[2] Hohl, G.-F. (1992). p-V-T Behaviour of the Alkali Metals Caesium, Rubidium and Potassium Near their Liquid-Gas Phase Transition Up to the Critical Point: Experimental Results for Potassium, *Ph. D. Thesis*, University of Marburg, Germany (in German).
[3] Hodgson, W. M. (1978). Equation of State and Transport Measurements on Expanded Liquid Metals up to 8000 K and 0.4 GPa, *Ph. D. Thesis*, University of California, U.S.A.
[4] Seydel, U., Fucke, W. and Wadle, H. (1980). Die Bestimmung thermophysika-lischer Daten flüssiger hochschmelzender Metalle mit schnellen Pulsaufheizexperimenten (Verlag Dr. Peter Mannhold, Düsseldorf, Germany).
[5] Pottlacher, G. (1987). Bestimmung thermophysikalischer Daten von Metallen bis in den Überhitzungsbereich der flüssigen Phase, *Ph. D. Thesis*, Technical University Graz, Austria.
[6] Martynyuk, M. M. (1992). *Thermochimica Acta*, **206**, 55.
[7] Hess, H., Kaschnitz, E. and Pottlacher, G. (1994). *High Pressure Research*, **12**, 29.

[8]   Likalter, A. A. (1985). *Teplofiz. Vys. Temp.*, **23**, 465 (in Russian).

[9]   Likalter, A. A. (1996). *Phys. Rev.*, **B53**, 4386.

[10] Hess, H. (1995). *Phys. Chem. Liq.*, **30**, 251.

[11] Hess, H. and Schneidenbach, H. (1996). *Z. Metallkd.*, **87**, 979.

[12] Franz, G. (1980). Measurement of Structure, Electrical Conductivity and PVT Data of Alkali Metals Up to 2100 K at Higher Pressure, *Ph. D. Thesis*, Univerisity of Marburg, Germany (in German).

[13] Ben-Yosef, N. and Rubin, A. G. (1969). *Phys. Rev. Lett.*, **23**, 289.

[14] DeSilva, A. W. and Kunze, H.-J. (1994). *Phys. Rev.*, **E49**, 4448.

[15] Krisch, I., Schmieder, E. and Kunze, H.-J. (1995). In: *Proc. Int. Conf. Phys. Strongly Coupled Plasmas*, (Eds.) Kraeft, W. D. and Schlanges, M. (World Scientific, Singapore) pp. 234–239.

[16] Kloss, A., Motzke, T., Grossjohann, R. and Hess, H. (1996). *Phys. Rev.*, **E54**, 5851.

[17] Likalter, A. A. (1992). *Sov. Phys. Usp.*, **35**, 591.

[18] Ziman, J. M. (1979). *Models of Disorder* (Cambridge University Press, Great Britain).

[19] Hoshino, H., Schmutzler, R. W., Warren, W. W. and Hensel, F. (1976). *Phil. Mag.*, **33**, 255.

[20] Hoshino, H., Schmutzler, R. W. and Hensel, F. (1976). *Ber. Bunsenges. Phys. Chem.*, **80**, 27.

[21] Kloss, A., Hess, H. and Schneidenbach, H. (1997). *High Temp. -High Press.*, **29**, 215.

[22] Likalter, A. A. (1988). *Sov. Phys. JETP*, **67**, 2478.

[23] Joffe, A. F. and Regel, A. R. (1960). *Prog. Semicond.*, **4**, 237.

[24] Hultgren, R., Desai, P. D., Hawkins, D. T., Gleiser, M., Kelley, K. K. and Wagman, D. D. (1973). *Selected Values of the Thermodynamic Properties of the Elements*, (American Society for Metals, Metals Park, Ohio).

[25] Kubaschewski, O., Alcock, C. B. and Spencer, P. J. (1993). *Materials Thermochemistry*, (Pergamon Press, Oxford).

[26] Iida, T. and Guthrie, R. I. L. (1993). *The Physical Properties of Liquid Metals* (Clarendon Press, Oxford).

[27] Likalter, A. (1997). *Physica Scripta*, **55**, 114.

[28] Götzlaff, W., Schönherr, G. and Hensel, F. (1988). *Z. Phys. Chem. Neue Folge*, **156**, 219; Götzlaff, W. (1988). *Ph. D. Thesis*, University of Marburg, Germany (in German).

[29] Young, D. A. (1977). *A Soft Sphere Model for Liquid Metals*, (Lawrence Livermore Laboratory Report UCRL-52 352, University of California, U.S.A.)

[30] McGonigal, P. J., Kirshenbaum, A. D. and Grosse, A. V. (1962). *J. Phys. Chem.*, **66**, 737.

[31] Morris, E. (1964). *An Application of the Theory of Corresponding States to the Prediction of the Critical Constants of Metals*, (AWRE Report No. 0-67/64, United Kingdom Atomic Energy Authority).

[32] Hensel, F. and Franck, E. U. (1966). *Ber. Bunsenges. Phys. Chem.*, **70**, 1154 (in German).

[33] Young, D. A. and Alder, B. J. (1971). *Phys. Rev.*, **A3**, 364.

[34] Fortov, V. E., Dremin, A. N. and Leontyev, A. A. (1974). *Teplofiz. Vys. Temp.*, **13**, 1072 (in Russian).

[35] Rau, H. (1974). *J. Chem. Thermodynamics*, **6**, 525.

[36] Alekseev, V. A., Ovcharenko, V. G., Ryzhkov, Yu. F., Niselson, L. A. and Zakharov-Cherenkov, V. K. (1975). *High Temp. - High Press.*, **7**, 676.

[37] Fischer, R., Schmutzler, R. W. and Hensel, F. (1980). *J. Non-Crystalline Solids*, **35 and 36**, 1295.

[38] Martynyuk, M. M. (1989). *Parameters of the Critical Points of Metals*, People's Friendship University, Moscow (in Russian).

[39] Krisch, I. and Kunze, H.-J. (1997). *Verh. DPG*, Mainz, p. 278; Kloss, A., Rakhel, A. and Hess, H. (1997). *Verh. DPG*, Mainz, p. 278.

[40] Redmer, R., Reinholz, H., Röpke, G., Winter, R., Noll, F. and Hensel, F. (1992). *J. Phys. Condens. Matter*, **4**, 1659; Reinholz, H. and Redmer, R. (1993). *J. Non. Cryst. Solids*, **156–158**, 654.